

RESEARCH ARTICLE

Study on the Prediction Model of Swelling Response of EPDM in Liquid Mixture by Using the Modified Flory–Huggins Interaction Parameter (χ_{HSP})

Zhuozhuo Li | Guangyong Liu 

Key Laboratory of Rubber-Plastics, Ministry of Education/Shandong Provincial Key Laboratory of Rubber-Plastics, Qingdao University of Science & Technology, Qingdao, P. R. China

Correspondence: Guangyong Liu (liuguangyong@qust.edu.cn)

Received: 7 August 2024 | **Revised:** 17 December 2024 | **Accepted:** 30 December 2024

Funding: The authors received no specific funding for this work.

ABSTRACT

The swelling responses of ethylene propylene diene monomers (EPDM) in cyclohexane/xylene (CYH/X) and cyclohexane/cyclohexanone (CYH/C) binary systems were studied by using equilibrium swelling method, and the co-solvent effect was further analyzed. The results show that the swelling responses of EPDM in CYH/X and CYH/C binary systems are significantly different. EPDM exhibits more obvious co-solvent effect in CYH/C binary system which may be generated by the self-association of cyclohexanone. In addition, the modified Flory–Huggins interaction parameter (χ_{HSP}) calculated by three-dimensional solubility parameters (HSP) was used to establish the prediction model from the correlation with the swelling ratio (q_m) of EPDM. The prediction model can be represented by an exponential equation with high degree of fitting, and the calculated q_m values from this model are comparable with the experimental values. The prediction model has been employed to evaluate the swelling responses (q -fitting) of EPDM in IRM 903 test oil/ethanol mixtures theoretically. It reveals that lower χ_{HSP} values result in higher swelling responses of EPDM, following the same rule of q - χ_{HSP} . Potentially, the prediction model based on χ_{HSP} provides a new way to determine the swelling responses of EPDM based rubber parts in any possible fluids.

1 | Introduction

As one of the important parameters to measure the compatibility between substances, solubility parameters have been widely used in polymer-related fields, such as the calculation of phase equilibrium of multicomponent systems, the selection of polymer plasticizing systems, and the prediction of polymer solubility [1]. As the basis for selecting solvents and additives in rubber and coating industry, solubility parameters also play an important role in predicting the compatibility of materials [2]. The solubility parameter (δ) was proposed by Hildebrand et al. in the middle of the 20th century and defined as the square root of the cohesive energy density, which was an important parameter to characterize the interaction strength of simple liquid molecules

[3, 4]. The Hildebrand solubility parameter is a relatively single value, which can accurately characterize the solubility of non-polar polymer. However, the intermolecular force of polar polymer becomes more complex, resulting in big errors of the Hildebrand solubility parameter and limitations of its further application [5–8]. For this reason, Hansen proposed a three-dimensional solubility parameter based on the one-dimensional solubility parameter (δ) by dividing it into three different parts: dispersion force component (δ_d), polar force component (δ_p), and hydrogen bonding force component (δ_h) [9–12], as shown in Equation (1):

$$\delta_t^2 = \delta_d^2 + \delta_p^2 + \delta_h^2 \quad (1)$$

HSP value provides a convenient method for studying and predicting the interaction of polymer–polymer and polymer–low molecular substances [13]. This interaction can be qualitatively reflected by the energy difference (R_a), that is, the distance from the small molecule to the center of the polymer sphere, as shown in Equation (2):

$$R_a = \left[4 \times (\delta_a^p - \delta_d^s)^2 + (\delta_p^p - \delta_p^s)^2 + (\delta_h^p - \delta_h^s)^2 \right]^{1/2} \quad (2)$$

Since the Flory–Huggins interaction parameter (χ) was proposed, it has been used to study the interaction between solvent and polymer, and good results have been obtained [14]. For strict non-polar systems, the traditional Flory–Huggins interaction parameters (χ_T) can be calculated by correspondence theory and Hildebrand solubility parameters, as shown in Equation (3):

$$\chi_T = 0.34 + \frac{V}{RT} (\delta_p - \delta_s)^2 \quad (3)$$

where the constant 0.34 is the entropy correction term, δ_p and δ_s are the Hildebrand solubility parameters of polymer and solvent, T is the absolute temperature, V is the molar volume of solvent, and R is the gas constant.

However, for polar systems with polarity and hydrogen bonding effects, a new modified Flory–Huggins interaction parameter (χ_{HSP}) is needed to replace the traditional one [15–19], as shown in Equation (4):

$$\chi_{HSP} = \frac{V}{4RT} R_a^2 \quad (4)$$

Equation (4) connects the Flory–Huggins interaction parameter with the HSP values of polymer–solvent by considering the molecular size of solvent, temperature, and the interaction forces between polymer and solvent.

Ethylene propylene diene monomer (EPDM) is a random copolymer copolymerized by ethylene, propylene, and a small amount of conjugated diene [20]. As a highly saturated non-polar rubber material, the unsaturated bonds exist only in the side chain, which brings EPDM with good ozone resistance, heat resistance, and polar solvent resistance and makes it widely used as automotive parts, building materials, wires, and cables [21–26]. The application of EPDM makes it inevitably face some liquid environment, which has great impacts on the life of rubber products. Furthermore, volume expansion will lead to the decline of properties of rubber products, and thus, the study of the resistance to solvent has important scientific and practical meanings.

In the past work, researchers have studied the swelling behaviors and Flory–Huggins interaction parameters (χ) of many rubber materials. Southern studied the swelling behavior of natural rubber under two-dimensional compression and found that the surface resistance of rubber deviated from the predicted value [27]. Varghese studied the swelling behavior of

natural rubber in n-alkane solvents such as pentane, n-hexane, n-heptane, and octane and found that sisal fiber limited the swelling degree of natural rubber [28]. Liu calculated the χ_{3D} between nitrile butadiene rubber and different solvents and found that the swelling degree of nitrile butadiene rubber decreased with the increase of χ_{3D} [29]. Díez determined the solubility parameters of SBS with different structures by inverse gas chromatography and calculated the interaction parameters between rubber and solvent. It was found that the interaction parameter theory has important guiding value for simulating the separation steps in the process of rubber synthesis [30]. P.C.Prakash studied the effect of the modified nano-ferrocene oxide on the swelling behavior of EPDM/SBR nanocomposites and found that the degree of swelling decreased with the increase of nano-filler content for the nanocomposites filled EPDM/SBR composites [31]. According to Flory–Rehner relation and Lorenz–Park equation, Maria Daniela Stelescu analyzed the interaction between EPDM and hemp fiber based on equilibrium swelling measurement. It was found that the swelling degree of EPDM/hemp fiber was affected by hemp content, and the EPDM sample with the highest hemp fiber content had the highest degree of swelling [32].

Up to now, studies on the solvent resistance were mainly focused on single solvent, and rarely investigation referred to the solvent mixture. In this work, the swelling responses of EPDM vulcanizates in cyclohexane/xylene (non-polar/non-polar) and cyclohexane/cyclohexanone (non-polar/polar) binary systems at different temperatures were studied by equilibrium swelling test [33–35]. The swelling characteristics and co-solvent effects of EPDM vulcanizates in the binary systems were analyzed. Besides, χ_{HSP} values were used to correlate the swelling responses (q_m) of EPDM for the purpose of determining the prediction model. Finally, it was attempted to adopt this prediction model to investigate the swelling responses of EPDM in IRM 903/Ethanol quantitatively.

2 | Experimental

2.1 | Materials and Formulations

The raw rubber used in this work was EPDM with the ethylene content of 52wt%, ENB content of 9wt% and Mooney viscosity (ML1+8, 50°C) of 66 and was provided by ARLANXEO (The Hague, the Netherlands). The vulcanization system, including peroxide crosslinking agent (Dicumyl peroxide) and co-agent (Triallyl isocyanurate), was supplied by ARKEMA (Paris, France). The solvents included cyclohexane (density: 0.780g/cm³, molar volume: 108.9 cm³/mol, boiling point 80.7°C), xylene (density: 0.865g/cm³, molar volume: 121.1 cm³/mol, boiling point: 137°C), and cyclohexanone (density: 0.947g/cm³, molar volume: 104.2 cm³/mol, boiling point: 155°C) and were provided from Sigma-Aldrich (Saint Louis, MO, the USA). A simplified formula (EPDM 100 phr, dicumyl peroxide 6 phr, triallyl isocyanurate 2 phr) was selected to prepare EPDM vulcanizate for the purpose of reducing the experimental error resulting by the effects of other components.

2.2 | Sample Preparation and Swelling Test

The temperature of the two-roll open mill (BL-6175, BOLON Precision Testing Machines Co. Ltd. China) was first set as 50°C with the roll speed ratio of 1:1.2. Then, the vulcanization system was added after plasticization of EPDM, and 5 min was further needed for the mixing to get the EPDM compound with uniformly dispersed vulcanization system. Finally, vulcanized samples with a thickness of 2 mm were prepared by a plate curing machine (XLB, Qingdao Yadong Rubber Machinery Co. Ltd. China). The pressure was 10 MPa, the temperature was 175°C, and the curing time was 13 min which was determined from the curing curve. Two different binary solvent mixtures, cyclohexane/xylene (CYH/X) and cyclohexane/cyclohexanone (CYH/C), were prepared for equilibrium swelling experiments, where CYH/X was the non-polar/non-polar binary system and CYH/C was the non-polar/polar binary system. The proportions of the two solvent mixture systems were 100/0, 75/25, 50/50, 25/75, and 0/100, respectively, and the three-dimensional solubility parameters were shown in Table 1.

2.2.1 | Swelling Test

Cylindrical samples with the diameter of 2 cm and thickness of 2 mm were cut out from the vulcanized film and immersed in acetone at room temperature to extract the uncrosslinked ingredients and low molecular substances from the samples. First, the extracted samples were weighed as the initial mass for the swelling test (W_0), then the samples were immersed in CYH/X and CYH/C solvent mixtures for the diffusion tests. At periodic intervals, the immersed samples were taken out and weighed immediately (W_t). After weighing, the samples were put back into the mixtures, and such operations were carried out several times until the equilibrium swelling state was reached. The final weight of the swollen samples at equilibrium states was recorded as W_f . The temperatures for these diffusion tests were 25°C, 35°C, 45°C, and 55°C, respectively. Five samples were selected for each test to reduce the weighing error.

The maximum swelling ratio q_m , the ratio of the volume of the swollen sample to the initial sample can be calculated by using the following Equation (5):

$$q_m = \frac{(W_f - W_0) / \rho_a + W_0 / \rho_b}{W_0 / \rho_b} \quad (5)$$

where ρ_a and ρ_b are the densities of the solvent and EPDM sample, respectively.

3 | Results and Discussion

3.1 | Swelling Characteristics of EPDM in Solvent Mixtures

First, the effect of swelling temperature the swelling behaviors of EPDM vulcanizates in CYH/X and CYH/C binary systems were studied, and the results are shown in Figures 1 and 2.

It can be seen from Figure 1 that the maximum swelling ratio (q_m) of EPDM is reached within 2000 min, which remains basically unchanged with the extension of swelling time. In addition, the swelling rates (slope at the initial stage of swelling) of EPDM stay consistent basically in the CYH/X binary system for different ratios. However, the swelling temperature and the volume ratio of cyclohexane to xylene have obvious effects on the q_m values. The increase in q_m (Δq) is 0.36 at the swelling temperature of 25°C (Figure 1A). When the swelling temperatures are 35°C, 45°C, and 55°C, the Δq values are 0.30 (Figure 1B), 0.29 (Figure 1C), and 0.22 (Figure 1D), respectively. In other words, the increase in q_m of EPDM vulcanizate becomes smaller with increasing swelling temperature.

Figure 2 shows the swelling behaviors of EPDM in CYH/C binary system. It can be seen that the swelling rate and q_m value of EPDM in the CYH/C binary system increase with the decrease of cyclohexanone content. The q_m value of EPDM in the pure cyclohexanone is small due to the poor compatibility caused by

TABLE 1 | Three-dimensional solubility parameters of the binary solvent mixtures.

Solvent mixture	Molecular structure	Volume ratio	δ_d , MPa $^{1/2}$	δ_p , MPa $^{1/2}$	δ_h , MPa $^{1/2}$
Cyclohexane:Xylene		0:100	17.8	1	3.1
		25:75	17.55	0.75	2.375
		50:50	17.3	0.5	1.65
		75:25	17.05	0.25	0.925
		100:0	16.8	0	0.2
Cyclohexane:Cyclohexanone		0:100	17.8	8.4	5.1
		25:75	17.55	6.3	3.875
		50:50	17.3	4.2	2.65
		75:25	17.05	2.1	1.425
		100:0	16.8	0	0.2

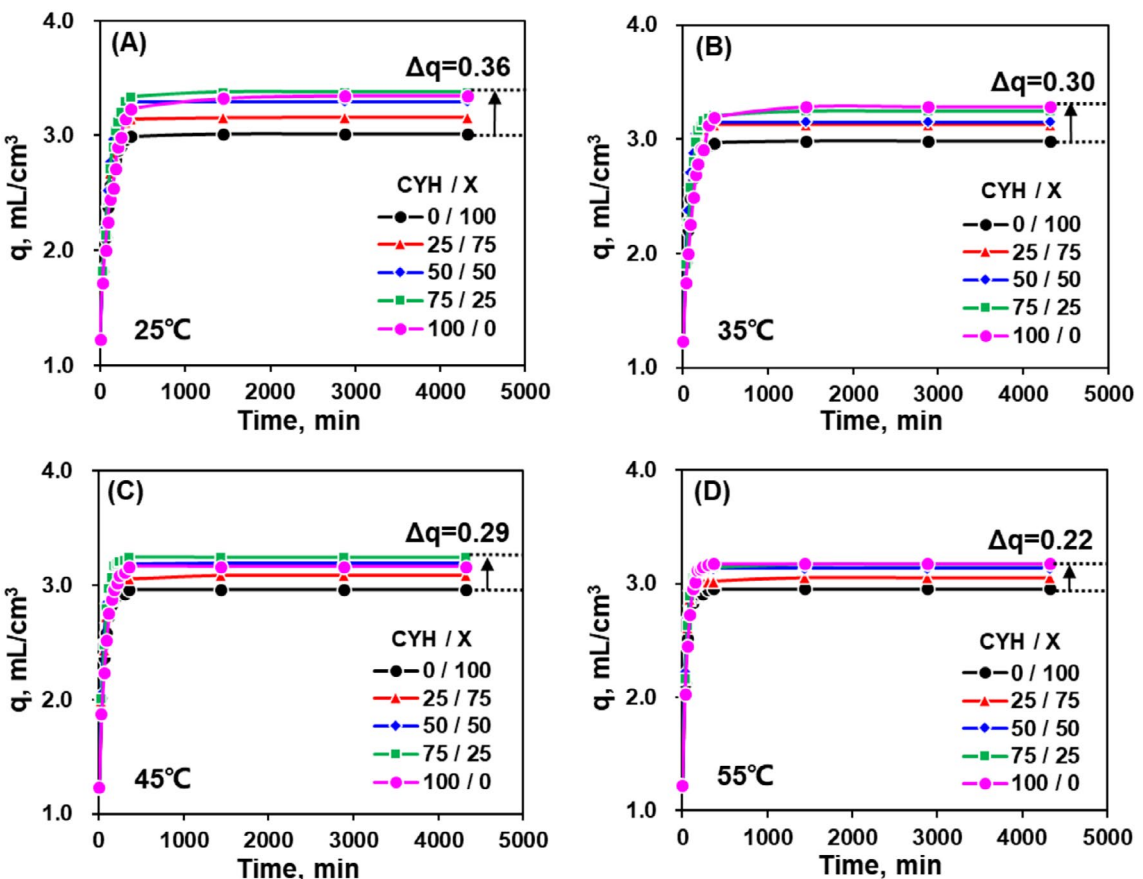


FIGURE 1 | Swelling behaviors of EPDM vulcanizates in CHY/X binary system at incremental temperature: (A) $T=25^{\circ}\text{C}$, (B) $T=35^{\circ}\text{C}$ (C) $T=45^{\circ}\text{C}$, (D) $T=55^{\circ}\text{C}$. [Color figure can be viewed at wileyonlinelibrary.com]

the difference of polarity between EPDM and cyclohexanone. The decrease in polarity of CYH/C binary system caused by mixing cyclohexane into cyclohexanone leads to better compatibility with EPDM, and the q_m value of EPDM increases consequently. The swelling temperature has no obvious effect on the change trend of q but affects the increasing amplitude of q value of EPDM in CYH/C binary system. Furthermore, the downtrend of Δq with temperature is similar with that of CYH/X binary system, and the Δq values are 1.8 (Figure 2A), 1.7 (Figure 2B), 1.4 (Figure 2C), and 1.4 (Figure 2D) when the swelling temperature are 25°C , 35°C , 45°C , and 55°C , respectively. However, the Δq values between the two binary systems are quite different.

3.2 | Cosolvent Effects of EPDM in Binary Systems

Further analysis of Figures 1 and 2 shows that there is a significant difference in the swelling behavior of EPDM in CYH/X and CYH/C binary systems, which may be caused by the different properties of the two mixed solvents. In addition, it can be seen that the q_m value may show a non-linear trend with the change in the composition of mixed solvents. It is assumed that there is a linear additivity between the swelling ratio and the composition of the mixed solvents, that is:

$$q_{\text{cal}} = q_1 x_1 + q_2 x_2 \quad (6)$$

where q_{cal} is the maximum swelling ratio calculated theoretically, q_1 and q_2 are the maximum swelling ratios of EPDM in

pure solvent 1 and 2, respectively, and x_1 and x_2 are the volume fractions ($x_1 + x_2 = 1$) of solvent 1 and 2 in the binary system, respectively.

The relationship between the experimental q_m value and the composition of CYH/X and CYH/C binary systems is shown in Figure 3.

For the CYH/X binary system (Figure 3A), at the swelling temperature of 25°C , q_m value increases first and then decreases with increasing the volume fraction of xylene, showing a non-linear relationship. Herein, the difference between the experimental q_m value and the theoretical calculated q_{cal} value is defined as Δq , which represents the increase of the maximum swelling ratio of EPDM in the binary system. EPDM reaches the maximum q_m value when the volume fraction of xylene is between 20% and 40% for CHY/X binary system. The change of q_m value at swelling temperature of 45°C (blue solid line in Figure 3A) is similar with that at 25°C , but q_m decreases with swelling temperature. Further observation on the swelling temperatures of 35°C and 55°C reveals that the q_m value decreases nonlinearly with the increase of xylene content and no maximum q_m appears in the whole range of composition.

For the CYH/C binary system (Figure 3B), the q_m value shows a non-linear downward trend with the increase of cyclohexanone content and no peak value emerging in the overall range of composition. However, EPDM shows remarkable cosolvent

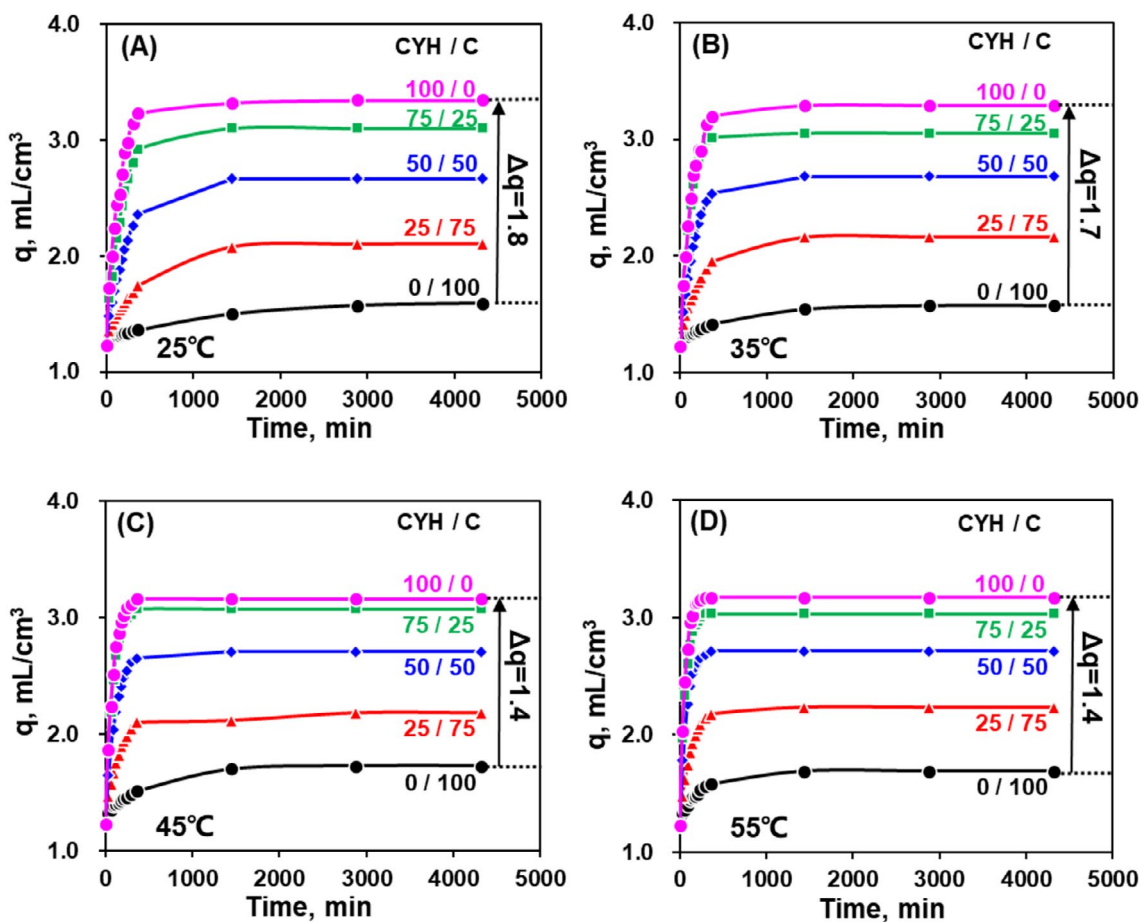


FIGURE 2 | Swelling behaviors of EPDM vulcanizates in CHY/C binary system at incremental temperature: (A) $T=25^{\circ}\text{C}$, (B) $T=35^{\circ}\text{C}$ (C) $T=45^{\circ}\text{C}$, (D) $T=55^{\circ}\text{C}$. [Color figure can be viewed at wileyonlinelibrary.com]

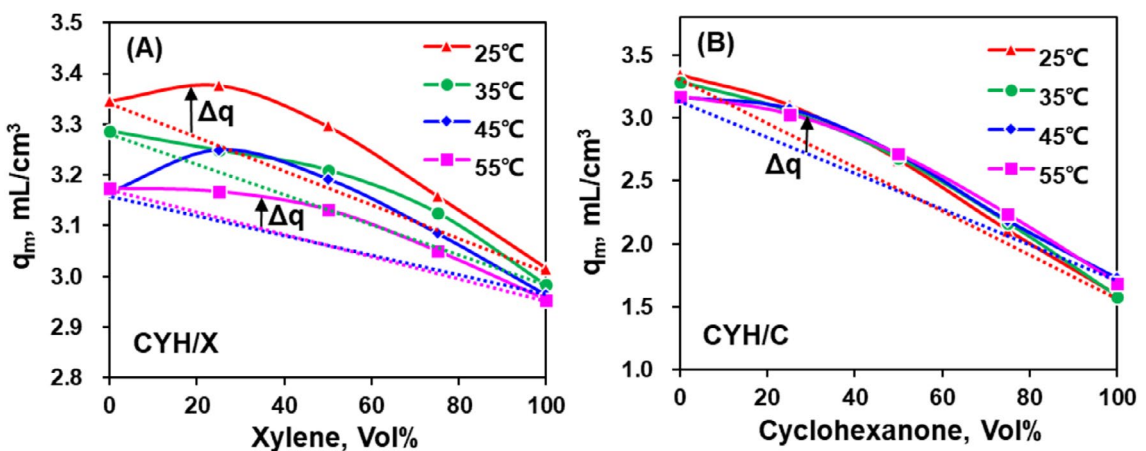


FIGURE 3 | Relationship between q_m and composition: (A) CYH/X binary system, (B) CYH/C binary system. [Color figure can be viewed at wileyonlinelibrary.com]

effect, that is, the Δq value is larger in the CYH/C binary system. The swelling temperature exerts a more complex influence on q_m value with the volume fraction of cyclohexanone being 40% as the demarcation point. q_m exhibits a higher value at lower swelling temperature when the volume fraction of cyclohexanone is less than 40%. This may be due to the fact that cyclohexane, as a good solvent for EPDM, accounts for a large proportion in the mixture ($> 60\%$) and causes the crosslinking

network of EPDM to dilate completely even at 25°C . At the same time, the crosslinking bond produces a certain retraction force, and the dynamic swelling equilibrium achieves when the retraction force is equal to dilation force. Although the movements of both solvent molecules and EPDM macromolecular chains become faster at incremental swelling temperature, the retraction force also increases, and thus, the q_m value decreases at higher swelling temperature.

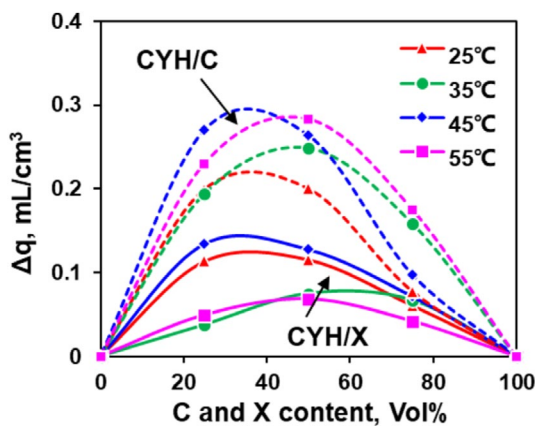


FIGURE 4 | Correlations of Δq with the compositions of CYH/C (dotted lines) and CYH/X (solid lines) binary systems. [Color figure can be viewed at wileyonlinelibrary.com]

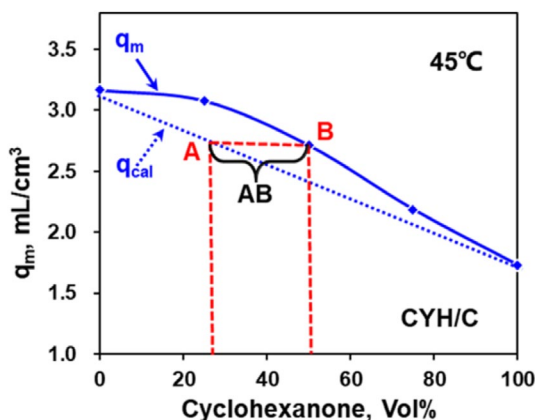


FIGURE 5 | Self-association of cyclohexanone in the CYH/C binary system. [Color figure can be viewed at wileyonlinelibrary.com]

On the contrary, q_m has a higher value at higher swelling temperature when the volume fraction of cyclohexanone is more than 40%, which may be due to the fact that the association effect generated between polar cyclohexanone molecules makes it difficult to enter the EPDM crosslinking network. Increasing

swelling temperature breaks the associations, and the movement of the cyclohexanone molecules becomes stronger. Under such conditions, there are more cyclohexanone molecules entering the EPDM crosslinking network, and thus resulting in further increase of the q_m value at higher swelling temperature.

The physical meaning of Δq discussed above represents the magnitude of the cosolvent effect of EPDM vulcanizate in the mixed solvent system. Plotting Δq against the composition (Figure 4) shows that the cosolvent effects (Δq) of EPDM in both CYH/C and CYH/X binary systems increase first and then decrease with the change of composition. Further comparison of the results shows that CYH/C binary system (dashed lines) exhibits greater cosolvent effect than that of CYH/X binary system (solid lines). It is because the cyclohexanone molecules show self-association states due to the strong dipole moment effects, and thus, the swelling of EPDM vulcanizate in pure cyclohexanone solvent is relatively low. When cyclohexane is added, the self-association state of cyclohexanone is disturbed to a certain extent, and the dissociated cyclohexanone molecules show higher diffusivity and easier to enter into the EPDM crosslinking network. Macroscopically, it shows a greater cosolvent effect with higher temperature. Taking the swelling temperature of 45°C as an example, the degree of self-association of cyclohexanone is analyzed, as shown in Figure 5.

As obtained from the experiment, the high polarity and strong self-association state make it difficult for pure cyclohexanone molecules to enter the crosslinking network and thus generate low swelling response of EPDM. Assuming that there is a linear additivity of the swelling ratio, that is, cyclohexane and cyclohexanone swell the EPDM sample in proportion, then the theoretical swelling ratio (q_{cal}) can be calculated linearly as shown in Figure 5 (blue dashed line). The actual swelling curve of EPDM vulcanizate is shown by the blue solid line (q_m), which is higher than q_{cal} value, and the difference (Δq) between q_m and q_{cal} is regarded as the cosolvent effect. The q_m value at 50% cyclohexanone is recorded as point B, and the intersection point A on the theoretical swelling curve is obtained by a horizontal line from point B to q_{cal} curve. Then, the cyclohexanone content relating to point A is 28%. Meaning that the experimental q_m value at cyclohexanone content of 50% equals to the calculated q_{cal} value with 28% cyclohexanone content. The difference of cyclohexanone

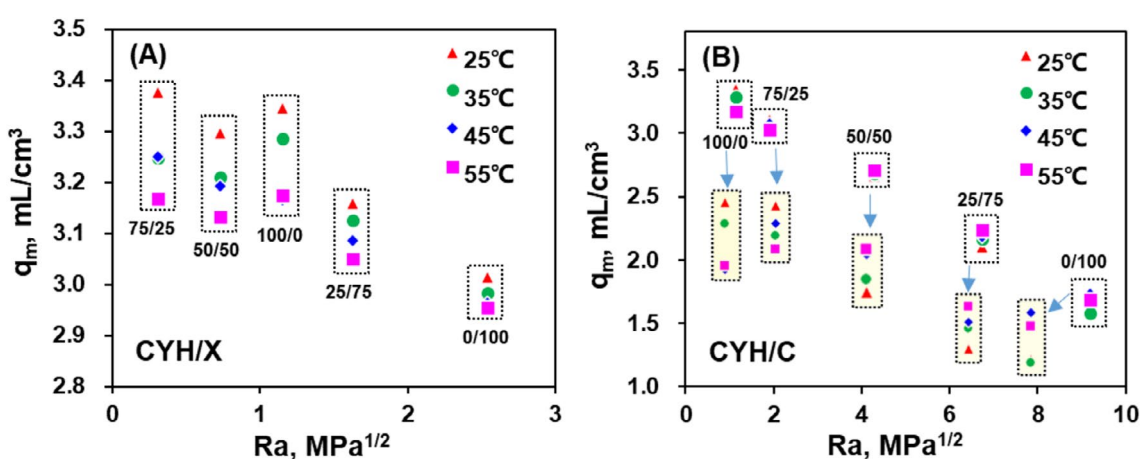


FIGURE 6 | Correlation q_m with R_a : (A) CYH/X binary system; (B) CYH/C binary system. [Color figure can be viewed at wileyonlinelibrary.com]

content between point A and B is 22% (AB) can be considered as the proportion of the self-associating part of cyclohexanone. Of course, this hypothesis has not been proved in this work, and experimental test will be conducted to prove the rationality of this hypothesis in future work.

3.3 | Relationships of q_m With Ra and χ

The adsorption capacity of EPDM to each solvent component is different during swelling process, and the diffusion rates of solvents into the crosslinking network are also different. This phenomenon can be considered as the preferential adsorption of EPDM to solvents. There are many factors affecting the preferential adsorption, including type of rubber, molecular structure of solvent, polarity, and compatibility between rubber and solvent. These factors can be linked to Ra and χ values, the interaction between rubber and solvent. A prediction model of q_m in binary solvent systems is attempted to be made by Ra and χ values, respectively. Correlation of q_m with Ra is first explored, as shown in Figure 6.

The calculation of Ra value excludes the temperature factor, and thus, the q_m values at four different swelling temperatures correspond to the same Ra (the dotted box in Figure 6). Further analysis of the CYH/X binary system (Figure 6A) shows that Ra exhibits a minimum value at the volume ratio of CYH/X being 75/25, corresponding to the highest q_m value. On the contrary, the calculated Ra shows the highest value at the volume ratio of CYH/X being 0/100, which relates to the lowest q_m value. q_m decreases nonlinearly with the increase of Ra value. In the CYH/C binary system (Figure 6B), q_m decreases and the corresponding Ra increases with the increase of cyclohexanone content (the volume ratio of CYH/C from 100/0 to 0/100). In general, higher q_m value corresponds to lower Ra value, and Ra can be calculated to qualitatively estimate the swelling responses of EPDM in solvent mixtures.

In addition, the temperature dependences of q_m are different for CYH/X and CYH/C binary systems, that is, the change of q_m with the swelling temperature is different at the same Ra value (the dotted box in Figure 6). Therefore, further study of the effect

of swelling temperature on q_m value is made, and the result is shown in Figure 7.

For CYH/X binary system (Figure 7A), the q_m value decreases slightly with the increase of temperature at the same Ra value (fixed CYH/X ratio). For CYH/C binary system (Figure 7B), the q_m values also show linear trends with increasing temperature, but there is a downturn at the ratio of CYH/C higher than 75/25 and uptrend at the ratio of CYH/C lower than 75/25. It shows that the swelling response of EPDM is not only related to the type of liquid medium but also closely relates to the swelling temperature. The calculation of Ra only considers the molecular structure parameters of rubber and solvent instead of external factors, such as temperature and molar volume. Therefore, q_m is correlated with χ_{HSP} value to establish a prediction model for the purpose of determining the swelling response of EPDM quantitatively, as shown in Figure 8.

According to the change of q_m with χ_{HSP} shown in Figure 8, it can be estimated preliminarily that an exponential relationship could be fitted between q_m and χ_{HSP} values. Therefore, an exponential equation is made as follows:

$$q = 3.2 \times e^{(-0.81 \times \chi_{HSP})} R^2 = 0.9813 \quad (7)$$

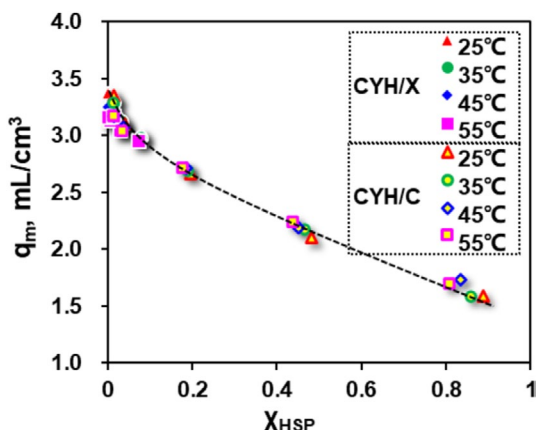


FIGURE 8 | Correlation q_m with χ_{HSP} for EPDM. [Color figure can be viewed at wileyonlinelibrary.com]

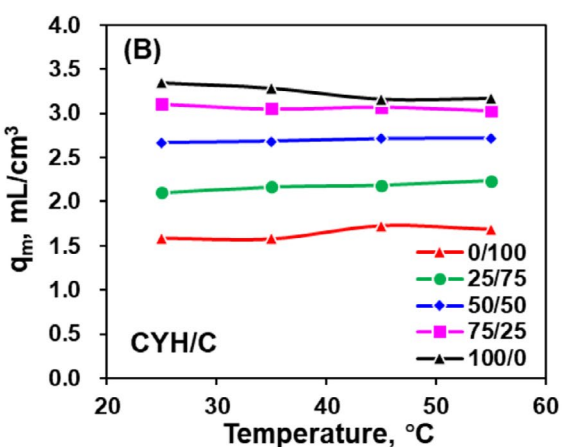
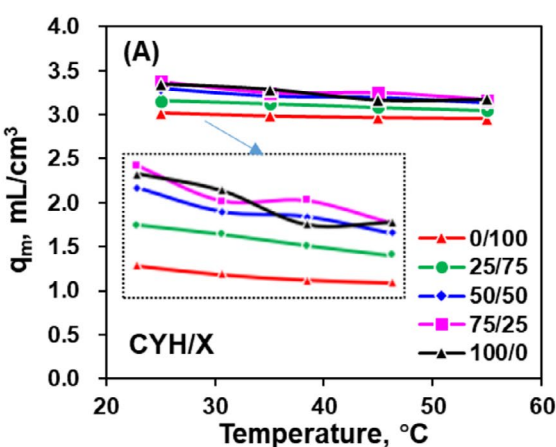


FIGURE 7 | Effects of swelling temperature on q_m : (A) CYH/X binary system; (B) CYH/C binary system. [Color figure can be viewed at wileyonlinelibrary.com]

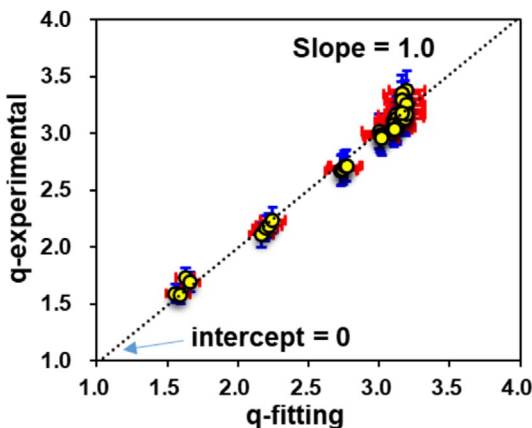


FIGURE 9 | Correlation of q_m between experimental and fitted values. [Color figure can be viewed at [wileyonlinelibrary.com](https://onlinelibrary.wiley.com)]

TABLE 2 | HSP values of IRM 903 and ethanol.

Fuels	δ_d , MPa $^{1/2}$	δ_p , MPa $^{1/2}$	δ_h , MPa $^{1/2}$	Vmol, mL/mol
IRM 903	17.9	0.7	1.8	350
Ethanol	15.8	8.8	19.4	58.6

This equation shows high degree of fitting (R^2 value), which is different from the linear relationship of nonpolar styrene-butadiene rubber [35, 36]. One of the main purposes of the theoretical calculated χ_{HSP} value is to predict the swelling behavior and liquid resistance of EPDM vulcanizates in different fluids. Herein, using the prediction model, the swelling ratios (q -fitting) of EPDM in all solvent mixtures are calculated and compared with the experimental values (q -experimental). The results are shown in Figure 9.

It can be seen from Figure 9 that there is a very good linear correlation between the experimental and theoretical fitting values with the slope of 1.0 and the intercept of 0. The calculated swelling ratios are comparable with the experimental values, which make it possible using HSP values to predict the swelling behaviors of EPDM vulcanizates in various liquids.

3.4 | Quantitative Prediction of Swelling Response in IRM 903/Ethanol

One of the possible applications of χ_{HSP} is the prediction of the swelling response of EPDM in the ever-emerging fuels and fluids. The reference oil IRM 903 (ASTM No. 3 oil) is one of the commonly used fluids in laboratory to evaluate the swelling response of rubber parts. However, IRM 903 is a mixture with the similar carbon atom composition as the “Naphtha high flash” substance, the HSP values of which have been determined in the same way as our previous work [29]. Some organic solvents, represented by ethanol, is frequently mixed with the bio-diesel to obtain bio-fuels with the consideration of exhaust gas emission and cost reduction. However, the composition and the resulting

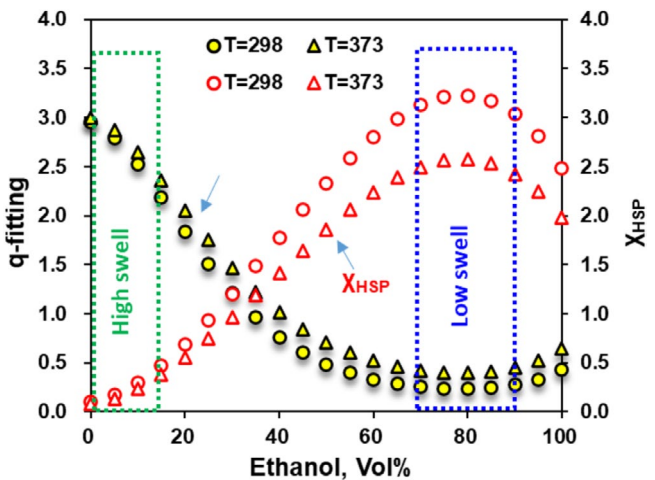


FIGURE 10 | Correlations of q -fitting and χ_{HSP} with ethanol content at different swelling temperatures. [Color figure can be viewed at [wileyonlinelibrary.com](https://onlinelibrary.wiley.com)]

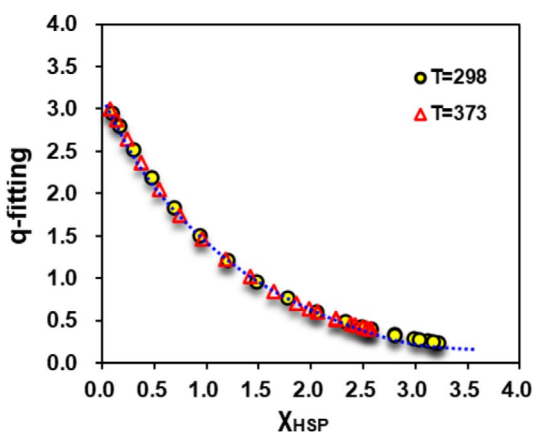


FIGURE 11 | Correlations of q -fitting with χ_{HSP} at different swelling temperatures. [Color figure can be viewed at [wileyonlinelibrary.com](https://onlinelibrary.wiley.com)]

HSP values will be changed accordingly for these new bio-fuel mixtures. Here, the HSP values of IRM 903 and ethanol are shown in Table 2.

Adding ethanol as the second component into IRM 903 gets a series of IRM 903/ethanol mixtures, and the HSP values of these mixtures follow a linear function of composition [29].

Herein, the swelling ratios (q -fitting) of EPDM in IRM 903/ethanol mixtures are calculated theoretically on the basis of the prediction model (Equation 7). In addition, the Flory-Huggins interaction parameters (χ_{HSP}) between EPDM and IRM 903/ethanol mixtures are calculated to correlate with ethanol content and q -fitting values. The results are depicted in Figures 10 and 11.

As shown in Figure 10, the q -fitting value decreases first and then increases with the increase of ethanol content, going through a low swell region. Accordingly, the χ_{HSP} value increases first and then decreases, passing through a minimum value. The low swell region relates well with the high χ_{HSP} value at the ethanol content from 70 vol% to 90 vol%.

Further observation on the relationship between q -fitting and χ_{HSP} (Figure 11) reveals that lower χ_{HSP} values generate higher swelling responses of EPDM, which follows the same rule of $q-\chi_{HSP}$. Meanwhile, the swelling temperature (298 K and 373 K) does not change this relationship but will affect the q and χ_{HSP} values. Potentially, the prediction model based on χ_{HSP} provides a new way to determine the swelling responses of EPDM based rubber parts in any possible fluids.

4 | Conclusion

The swelling temperature and the volume fraction show obvious effects on the q_m values of EPDM vulcanizates in CYH/C and CYH/X binary systems, but the swelling responses are different due to the different properties of the solvents. The self-association of cyclohexanone makes the CYH/C binary system exhibit a greater cosolvent effect than that of CYH/X binary system. Higher q_m value relates to lower Ra value, and q_m shows the highest value (Ra exhibits minimum value) for CYH/X binary system of 75/25. The q_m values show linear trends with increasing temperature for CYH/X and CYH/C binary systems. The swelling response is affected by the swelling temperature and molar volume as well, which are excluded during the calculation of Ra.

Through exponential fitting of q_m and χ_{HSP} values, a prediction model has been successfully established, and the swelling ratios of EPDM vulcanizates in all mixed solvents (q -fitting) have been calculated using the prediction model. The comparison with the experimental value (q -experimental) shows a very good linear correlation with the slope of 1 and the intercept of 0. The swelling ratios (q -fitting) of EPDM in IRM903/ethanol reference oils determined by the obtained prediction model indicate that the q -fitting decreases first and then increases with increasing ethanol content and a low swelling region occurs at the ethanol content from 70 vol% to 90 vol%. Accordingly, χ_{HSP} arises the opposite trend with q -fitting values. One can expect that the swelling responses in any known fluids can be predicted by taking advantage of the prediction model based on χ_{HSP} value.

Author Contributions

Zhuozhuo Li: conceptualization (supporting), data curation (supporting), formal analysis (supporting), investigation (supporting), visualization (supporting), writing – original draft (supporting). **Guangyong Liu:** methodology (supporting), project administration (supporting), resources (supporting), software (supporting), supervision (supporting), validation (supporting), writing – review and editing (supporting).

Ethics Statement

The authors have nothing to report.

Conflicts of Interest

The authors declare no conflicts of interest.

Data Availability Statement

The data that support the findings of this study are available from the corresponding author upon reasonable request.

References

1. M. Li, T. Ren, Y. Sun, et al., "New Parameter Derived From the Hansen Solubility Parameter Used to Evaluate the Solubility of Asphaltene in Solvent," *ACS Omega* 7 (2022): 13801–13807, <https://doi.org/10.1021/acsomega.2c00018>.
2. D. C. Santos, S. D. Filipakis, E. R. Lima, and M. L. Paredes, "Solubility Parameter of Oils by Several Models and Experimental Oil Compatibility Data: Implications for Asphaltene Stability," *Petroleum Science and Technology* 37 (2019): 1596–1602, <https://www.tandfonline.com/doi/full/10.1080/10916466.2019.1594288>.
3. G. Liu, M. Hoch, C. Wrana, K. Kulbaba, and G. Qiu, "A New Way to Determine the Three-Dimensional Solubility Parameters of Hydrogenated Nitrile Rubber and the Predictive Power," *Polymer Testing* 32 (2013): 1128–1134, <https://doi.org/10.1016/j.polymertesting.2013.07.001>.
4. R. Su, G. Liu, H. Sun, and Z. Yong, "A New Method to Measure the Three-Dimensional Solubility Parameters of Acrylate Rubber and Predict Its Oil Resistance," *Polymer Bulletin* 79 (2022): 971–984, <https://doi.org/10.1007/s00289-020-03516-6>.
5. M. Levin and P. Redelius, "Determination of Three-Dimensional Solubility Parameters and Solubility Spheres for Naphthenic Mineral Oils," *Energy & Fuels* 22 (2008): 3395–3401, <https://doi.org/10.1021/ef800256u>.
6. H. Li, X. Shi, X. Feng, and L. Dong, "Optimization Determination of Three-Dimensional Solubility Parameters of Fluororubber F2603," *IOP Conference Series: Materials Science and Engineering* 772 (2020): 012027, <https://doi.org/10.1088/1757-899X/772/1/012027>.
7. A. Alanazi, S. Alshehri, M. Altamimi, and F. Shakeel, "Solubility Determination and Three Dimensional Hansen Solubility Parameters of Gefitinib in Different Organic Solvents: Experimental and Computational Approaches," *Journal of Molecular Liquids* 299 (2020): 112211, <https://doi.org/10.1016/j.molliq.2019.112211>.
8. Y. Z. Wang, L. Y. Bi, H. J. Zhang, et al., "Predictive Power in Oil Resistance of Fluororubber and Fluorosilicone Rubbers Based on Three-Dimensional Solubility Parameter Theory," *Polymer Testing* 75 (2019): 380–386, <https://doi.org/10.1016/j.polymertesting.2019.03.004>.
9. X. Su, B. Shi, and L. Wang, "Investigation on Three-Dimensional Solubility Parameters for Explanation and Prediction of Swelling Degree of Polydimethylsiloxane Pervaporation Membranes," *Journal of Macromolecular Science, Part B* 54 (2015): 1248–1258, <https://doi.org/10.1080/00222348.2015.1085272>.
10. X. Jiang, X. Yuan, X. Guo, F. Zeng, and G. Liu, "Determination of Three-Dimensional Solubility Parameters of HNBR/EPDM Blends and the Transport Behaviors in Ester Solvents," *Journal of Applied Polymer Science* 139 (2022): e52881, <https://doi.org/10.1002/app.52881>.
11. M. Murase and R. Ohta, "Prediction of Molecular Affinity on Solid Surfaces via Three-Dimensional Solubility Parameters Using Interfacial Free Energy as Interaction Threshold," *Journal of Physical Chemistry C* 123 (2019): 13246–13252, <https://doi.org/10.1021/acs.jpcc.9b00154>.
12. Q. Liu, X. Shi, Y. Lu, and L. Dong, "Estimation of Three-Dimensional Solubility Parameters of DM-700 Polyester Resin by Turbidity Titration," *IOP Conference Series: Earth and Environmental Science* 384 (2019): 012069, <https://doi.org/10.1088/1755-1315/384/1/012069>.
13. S. Liu, Y. Jing, J. Tu, et al., "New Flory-Huggins Interaction Parameter Between SBR and p-Phenylenediamine Antioxidants and the Predictive Power in Molecular Structure and Rubber Formula Design," *Journal of Applied Polymer Science* 139 (2022): 51840, <https://doi.org/10.1002/app.51840>.
14. X. Jiang, X. Yuan, X. Guo, F. Zeng, H. Wang, and G. Liu, "Study on the Application of Flory–Huggins Interaction Parameters in Swelling Behavior and Crosslink Density of HNBR/EPDM Blend," *Fluid Phase Equilibria* 563 (2023): 113589, <https://doi.org/10.1016/j.fluid.2022.113589>.

15. J. D. Willis, T. M. Beardsley, and M. W. Matsen, "Simple and Accurate Calibration of the Flory-Huggins Interaction Parameter," *Macromolecules* 53 (2020): 9973–9982, <https://doi.org/10.1021/acs.macromol.0c02115>.

16. S. Antoine, Z. Geng, E. S. Zofchak, et al., "Non-intuitive Trends in Flory-Huggins Interaction Parameters in Polyether-Based Polymers," *Macromolecules* 54 (2021): 6670–6677, <https://doi.org/10.1021/acs.macromol.1c00134>.

17. M. A. Khansary, "Vapor Pressure and Flory-Huggins Interaction Parameters in Binary Polymeric Solutions," *Korean Journal of Chemical Engineering* 33 (2016): 1402–1407, <https://doi.org/10.1007/s11814-015-0277-6>.

18. Y. Aoki, S. Wu, T. Tsurimoto, et al., "Multitask Machine Learning to Predict Polymer-Solvent Miscibility Using Flory-Huggins Interaction Parameters," *Macromolecules* 56 (2023): 5446–5456, <https://doi.org/10.1021/acs.macromol.2c02600>.

19. M. Tambasco, J. E. G. Lipson, and J. S. Higgins, "Blend Miscibility and the Flory-Huggins Interaction Parameter: A Critical Examination," *Macromolecules* 39 (2006): 4860–4868, <https://doi.org/10.1021/ma060304r>.

20. C. Zhang, J. Wu, F. Teng, B. Su, Y. Wang, and H. Ao, "Theoretical and Experimental Characterization for Macro-Micro Friction Behaviors of EPDM Rubber," *Polymer Testing* 99 (2021): 107213, <https://doi.org/10.1016/j.polymertesting.2021.107213>.

21. L. Ma, W. Yang, and H. Guo, "Effect of Cross-Linking Degree of EPDM Phase on the Morphology Evolution and Crystallization Behavior of Thermoplastic Vulcanizates Based on Polyamide 6 (PA6)/ethylene-Propylene-Diene Rubber (EPDM) Blends," *Polymers* 11 (2019): 1375, <https://doi.org/10.3390/polym11091375>.

22. G. Zhang, X. Zhou, K. Liang, et al., "Mechanically Robust and Recyclable EPDM Rubber Composites by a Green Cross-Linking Strategy," *ACS Sustainable Chemistry & Engineering* 7 (2019): 11712–11720, <https://doi.org/10.1021/acssuschemeng.9b01875>.

23. H. Im and S. Jeoung, "Mechanical Aging Test and Sealing Performance of Thermoplastic Vulcanizate as Sealing Gasket in Automotive Fuel Cell Applications," *Polymers* 15 (2023): 1872, <https://doi.org/10.3390/polym15081872>.

24. J. Liu, X. Li, L. Xu, and T. He, "Service Lifetime Estimation of EPDM Rubber Based on Accelerated Aging Tests," *Journal of Materials Engineering and Performance* 26 (2017): 1735–1740, <https://doi.org/10.1007/s11665-017-2519-8>.

25. A. B. Bhattacharya, M. Das, T. K. Sreethu, P. Maji, and K. Naskar, "Influence of Different Mixing Sequence on UHMW-EPDM Based Thermoplastic Vulcanizates: Mechanical, Rheological and Morphological Characteristics," *Journal of Applied Polymer Science* 139 (2022): 52222, <https://doi.org/10.1002/app.52222>.

26. C. Li, Y. Wang, Z. Yuan, and L. Ye, "Construction of Sacrificial Bonds and Hybrid Networks in EPDM Rubber Towards Mechanical Performance Enhancement," *Applied Surface Science* 484 (2019): 616–627, <https://doi.org/10.1016/j.apsusc.2019.04.064>.

27. E. Southern and A. G. Thomas, "Effect of Constraints on the Equilibrium Swelling of Rubber Vulcanizates," *Journal of Polymer Science Part A: General Papers* 3 (1965): 641–646, <https://doi.org/10.1002/pol.1965.100030220>.

28. S. Varghese, B. Kuriakose, S. Thomas, and K. Joseph, "Effect of Adhesion on the Equilibrium Swelling of Short Sisal Fiber Reinforced Natural Rubber Composites," *Rubber Chemistry and Technology* 68 (1995): 37–49, <https://doi.org/10.5254/1.3538730>.

29. S. Liu, Y. Jing, J. Tu, H. Zou, Z. Yong, and G. Liu, "Systematic Investigation on the Swelling Behaviors of Acrylonitrile-Butadiene Rubber via Solubility Parameter and Flory-Huggins Interaction Parameter," *Journal of Applied Polymer Science* 139 (2022): 52172, <https://doi.org/10.1002/app.52172>.

30. E. Díez, G. Ovejero, M. D. Romero, and I. Díaz, "Polymer-Solvent Interaction Parameters of SBS Rubbers by Inverse Gas Chromatography Measurements," *Fluid Phase Equilibria* 308 (2011): 107–113, <https://doi.org/10.1016/j.fluid.2011.06.018>.

31. P. C. Prakash, D. Srinivasan, V. Navaneethakrishnan, and S. Vishvanathperumal, "Effect of Modified Nanographene Oxide Loading on the Swelling and Compression Set Behavior of EPDM/SBR Nano-Composites," *Journal of Inorganic and Organometallic Polymers and Materials* 34 (2024): 593–610.

32. M. D. Stelescu, A. Airinei, A. Bargan, et al., "Mechanical Properties and Equilibrium Swelling Characteristics of Some Polymer Composites Based on Ethylene Propylene Diene Terpolymer (EPDM) Reinforced With Hemp Fibers," *Materials* 15 (2022): 6838, <https://doi.org/10.3390/ma15196838>.

33. J. L. Valentín, J. Carretero-González, I. Mora-Barrantes, W. Chassé, and K. Saalwächter, "Uncertainties in the Determination of Cross-Link Density by Equilibrium Swelling Experiments in Natural Rubber," *Macromolecules* 41 (2008): 4717–4729, <https://doi.org/10.1021/ma8005087>.

34. V. S. Vinod, S. Varghese, and B. Kuriakose, "Assessment of Adhesion in Natural Rubber-Aluminium Powder Composites by Equilibrium Swelling in Aliphatic Solvents," *Journal of Materials Science* 35 (2000): 5699–5706, <https://doi.org/10.1023/A:1004810625113>.

35. H. Z. Chu, D. Liu, Z. W. Cui, K. Wang, G. X. Qiu, and G. Y. Liu, "Effect of Crosslink Density on Solubility Parameters of Styrene Butadiene Rubber and the Application in Pre-Screening of New Potential Additives," *Polymer Testing* 81 (2020): 106253, <https://doi.org/10.1016/j.polymertesting.2019.106253>.

36. S. S. Liu, X. P. Li, P. J. Qi, et al., "Determination of Three-Dimensional Solubility Parameters of Styrene Butadiene Rubber and the Potential Application in Tire Tread Formula Design," *Polymer Testing* 81 (2020): 106170, <https://doi.org/10.1016/j.polymertesting.2019.106170>.